A FUSION ALGORITHM FOR PATH PLANNING OF MOBILE ROBOTS IN ENVIRONMENTS WITH DYNAMIC OBSTACLES

Chongyang Lv*,**, Xuejie Fan*,**, and Mingxiao Sun***

Abstract

To find a smooth, safe global path that avoids the local dynamic obstacle, this article proposes a method of integrating the improved A* algorithm and artificial potential field method, namely, MAAPF. Firstly, the multi-objective functions are introduced into the heuristic function of the A* algorithm to reduce the redundant points in the global path. When the robot detects dynamic obstacles, it searches the global path node as the local goal according to the robot's position and detecting range, meanwhile combining the dynamic obstacle trajectory predicted by the autoregressive model and static obstacles in the detection range to construct the local map, then through the artificial potential field method that is improved by adding the goal guidance factor and gravitational distance threshold to complete local dynamic obstacle avoidance, avoid the goal is unattainable and locally optimal. The simulation demonstrates that improving the A* algorithm within a 3D environment and the artificial potential field algorithm has better results than other algorithms. Besides, the MAAPF can obtain a safe optimal path in circumstances with dynamic obstacles.

Key Words

Mobile robot, fusion path planning, MAAPF, dynamic obstacle avoidance

1. Introduction

Path planning takes into account factors, such as path length, energy consumption, and time elapsed to plan an optimal route from the starting position to the ending position, which as a key technology in robotics has been proverbially used in multifarious fields, such as the intelligent transportation systems, logistics systems, and search and rescue in disasters so on [1]–[3]. The general steps of path planning contain environment modelling and path search. Environment modelling is the basis of path search [4], and its main method includes the visible graph method [5], topology method, and grid method [6]. The path search can be separated into local route search and global route search according to the different environments in which the robot is located, global path planning relies on already known information to get the optimal path, it usually includes traditional algorithms, intelligent algorithms, graph-based approaches, and local path planning such as article potential filed and dynamic window method keeps away from the moving obstacle depending on the information acquired by sensors [7]–[11].

A* algorithm as a type of the global path planning algorithm is the most direct and impactful shortest pathfinding way [12]–[14]. A* algorithm explores the waypoint to the destination point by a heuristic function, reduces search blindness, and improves search efficiency by narrowing the scope of search [15]. There are countless studies on the path planning of the A* algorithm, [16] introduced the quadratic A* algorithm to reduce the length of the route and employed the dynamic tangential point method to adjust the concave and convex points to smooth the path. Reference [17] showed that the jump point search A* algorithm can find the route quickly yet there are still turning points resulting in a longer path compared with other modifications of the A* algorithm. Reference [18] considered introducing the weight information of the pavement into the heuristic formula, deleting the redundant points by turning points extraction strategy, and finally, finding the optimal path with small road roughness. Reference [19] used triangulation to deal with obstacles and generate Voronoi nodes as path points, then the priority of pathfinding and usual route nodes improved the A* algorithm.

* College of science, Harbin University of Science and Technology, Harbin, 150080, China; e-mail: lvchongyang@hrbust.edu.cn; chongyanglv@163.com; 879813389@qq.com

** Heilongjiang Provincial Key Laboratory of Optimization Control and Intelligent Analysis for Complex Systems, Harbin University of Science and Technology, Harbin, 150080, China.

*** College of Automation, Harbin University of Science and Technology, Harbin, 150080, China; e-mail: sunmingxiao@hrbust.edu.cn

Corresponding author: Chongyang Lv

Recommended by Reza Fotouhi
(DOI: 10.2316/J.2024.206-0882)

Artificial potential field as a pathfinding way is proposed by Khatib, its essence is a virtual force method. Reference [20] analysed the gravitational and repulsive potential field models, and pointed out that the artificial potential field method is easy to cause target unreachable problems and local extremums in a complex environment. Literature [21] avoids local optimisation by improving the repulsive potential field function and combined with directional escape. Owing to better obstacle avoidance, [22] and [23] took the artificial potential field to build heuristics factors in the ant colony algorithm, and [24] takes artificial potential field into account in the state transition rule, in the literature [25] obstacle avoidance is achieved by using the repulsion generated by the position and velocity of the obstacle.

However, when the robot is in a complex environment, the A* algorithm will occur the collision with the locomotor obstacles and generate more tutor points, and the artificial potential field will find an incomplete path owing to lacking awareness of global environmental information or fall into local optimal. Therefore, this paper base on mobile robot in land fuses global algorithms with local algorithms, constructs the multi-objective function to improve the A* algorithm, and rebuilds the potential function to mend the artificial potential field method, it contributes to the mobile robot completing obstacles avoidance behaviour and finds an optimal route in dynamic circumstances.

2. Improvements to the Algorithm

2.1 Environmental Model Description

Environment modelling is the basis for path planning, to effectively depict the environmental information and the state of the robot during the search path, this paper treats the robot as a point of motion on the plane and establishes a 3D environment map based on the grid method, the data stored in the grid reflects the environment of information.

The two-dimensional plane is partitioned into a grid of the same size R, with N rows and M columns, and the size of the robot determines the scale of the grid R. Assuming (x_i, y_i) is the coordinate of the ith grid, and the mapping relationship between the grid number and the coordinates is:

$$\begin{cases} x_i = R[\mathrm{mod}(i, M) - R/2] \\ y_i = R[N + R/2 - \mathrm{ceil}(i/N)] \end{cases} \tag{1}$$

To further build the 3D map, using the coordinates x and y to represent the rows and columns to form a 2D matrix, the z represents the height value and is used to reveal the inhomogeneity of the 2D plane. The terrain C is depicted as:

$$C_{\text{terrain}} = \begin{bmatrix} z_{11} & z_{12} & \dots & z_{1N} \\ z_{21} & z_{22} & \dots & z_{2N} \\ \dots & \dots & \dots & \dots \\ z_{M1} & z_{M2} & \dots & z_{MN} \end{bmatrix} \tag{2}$$

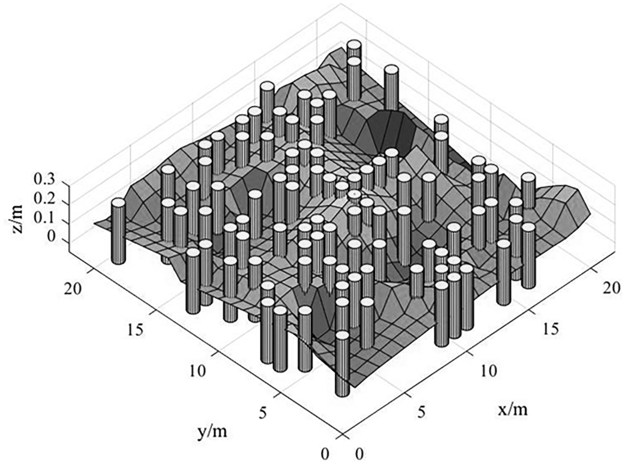

Figure 1. The map with the obstacles.

Meanwhile, regarding the obstacles in the environment as a series of cylinders with radius r, and the coordinate of the centre of each cylinder indicates the position of obstacle, and the final 3D environment map with the above obstacles is formed in Fig. 1.

2.2 The Improved A* Algorithm

The traditional A* algorithm can effectively handle most of the global planning problems, but there are a lot of redundant points in the optimisation results, which cause the zigzag path appears, and there is no doubt that this is not only detrimental to the action of the robot but also affects the effect of the algorithm. Reference [26] proposed a PSO-DV algorithm based on multi-objective optimisation, under its influence, based on the principle of traditional algorithms, the improvement of the A* algorithm also considers multi-objective optimisation. This method not only keeps the shortest path of the original algorithm but also completes the smoothing of the path, the specific improvements are as follows.

Firstly, when planning the robot's path, the robot needs to be abiding by the conditions described below:

I. The robot points to the target position in the process of deciding the next location from the current location. And the robot can detect obstacle in a very short time in its detection range and can quickly deal with the environment information obtained.

II. Each path point is independent, find the final path by extending N nodes, and deriving the overall cost function by calculating the cost function of each segment. All distances are expressed by Euclidean distances, for example, the distance $\rho(P, P_t)$ between node $P(x, y, z)$ and node $P_t(x_t, y_t, z_t)$ is presented as:

$$\rho(P, P_t) = \sqrt{(x - x_t)^2 + (y - y_t)^2 + (z - z_t)^2} \tag{3}$$

Under the above assumptions and conditions, we convert the robot path planning into a problem solved by a multi-objective optimisation method, as follows:

(i) *Path length function:*
Considering under the precondition that the starting and ending points are, respectively, (x_s, y_s, z_s), (x_t, y_t, z_t), the robot chooses the next point (x_i, y_i, z_i) as far away from the obstacles as possible at short notice, and when the route path is extended to the Nth node which means that the completed path is found, so the common objective function about the path length is determined as:

$$\begin{aligned} F_1 =& \sqrt{(x_1 - x_s)^2 + (y_1 - y_s)^2 + (z_1 - z_s)^2} \\ &+ \sum_{i=2}^{N-1} \sqrt{(x_i - x_{i-1})^2 + (y_i - y_{i-1})^2 + (z_i - z_{i-1})^2} \\ &+ \sqrt{(x_t - x_{N-1})^2 + (y_t - y_{N-1})^2 + (z_t - z_{N-1})^2} \end{aligned} \tag{4}$$

(ii) *Obstacle avoidance function:*
This function reveals the robot's ability to avoid obstacles, and assuming P_i is the ith nodes coordinate, using the nearest distance $D_{\min}(P_i)$ between P_i and the obstacles as well as the range of the obstacle to construct the obstacle avoidance function, it is defined as follows:

$$f_{2,i} = \begin{cases} k\left(\frac{1}{D_{\min}(P_i)} - \frac{1}{r}\right) & \text{if } D_{\min}(P_i) \le r \\ 0 & \text{otherwise} \end{cases} \quad i \in (1, 2, ..., N) \tag{5}$$

$$F_2 = \sum_{i=1}^{N} f_{2,i} \tag{6}$$

where r is the influence range of obstacle, k as a positive parameter to affect the value of obstacle avoidance function, $k = \frac{1}{2}$ in this article, the smaller the F_2, the safer the path found.

(iii) *Smoothness function*
Take the smoothness of the route as the third constraint function to obtain a smooth path. The robot generates a new path point during each extension, every two consecutive path points are connected to the target point to form two continuous line segments and convert the angle between the two segments into radians to indicate the smoothness of the route. The smoothing objective function is obtained as (7) and (8).

$$f_{3,i} = \arccos\left(\frac{(x_i - x_t)(x_{i-1} - x_t) + (y_i - y_t)(y_{i-1} - y_t) + (z_i - z_t)(z_{i-1} - z_t)}{\sqrt{(x_t - x_i)^2 + (y_t - y_i)^2 + (z_t - z_i)^2}\sqrt{(x_t - x_{i-1})^2 + (y_t - y_{i-1})^2 + (z_t - z_{i-1})^2}}\right) / \pi \tag{7}$$

$$F_3 = \arccos\left(\frac{(x_s - x_t)(x_1 - x_t) + (y_s - y_t)(y_1 - y_t) + (z_s - z_t)(z_1 - z_t)}{\sqrt{(x_t - x_s)^2 + (y_t - y_s)^2 + (z_t - z_s)^2}\sqrt{(x_t - x_1)^2 + (y_t - y_1)^2 + (z_t - z_1)^2}}\right) / \pi + \sum_{i=2}^{N} f_{3,i} \tag{8}$$

(iv) *Steering angle function*
In the process of the robot from one node to another, a large steering angle will increase the energy consumption and the time to find a path owing to the robot's physical maneuverability characteristics. Therefore, the three consecutive path nodes are connected in turn to form two consecutive line segments, and the steering angle θ is represented by the difference between the angle formed by these two lines segments and the horizontal plane, and the final steering angle constraint function which is constructed by combining the pre-set maximum steering angle constraint and can be demonstrated as:

$$\theta_i = \arctan\left(\frac{y_i - y_{i-1}}{x_i - x_{i-1}}\right) - \arctan\left(\frac{y_{i-1} - y_{i-2}}{x_{i-1} - x_{i-2}}\right) \quad i \in (2, 3, ..., N) \tag{9}$$

$$\alpha_i = |\theta_i| - \frac{\pi}{2} \tag{10}$$

$$f_{4,i} = \begin{cases} 1 & \text{if } \alpha_i \ge 0 \\ 0 & \text{else} \end{cases} \tag{11}$$

$$F_4 = \begin{cases} S + \sum_{i=1}^{N} f_{4,i} & \text{if } \sum_{i=1}^{N} f_{4,i} > 0 \\ 0 & \text{if } \sum_{i=1}^{N} f_{4,i} = 0 \end{cases} \tag{12}$$

where $\theta_i (i \in 2, 3, ..., N)$ is the turning angle of the ith node, $\theta_1 = 0$, and (x_0, y_0, z_0) represents the starting point in (9). Applying S ($S = 4$ in this article) to penalise the route where the node is located when the turning angle is greater than the 90°, the larger the cost function value, the more tortuous the final full path.

(v) *Slope angle function*
The angle between the line of two consecutive nodes and the horizontal plane is served as a slop angle cost function to express the diversification of the path in the vertical orientation, and the slope angle is restricted to the specified range to ensure that the mobile robot as stable as possible in movement and the flatness of path in the vertical plane. So the slope angle constraint function is expressed as

$$f_{5,i} = \begin{cases} 0 & \text{if } \beta_{\min} \le \beta_i \le \beta_{\max} \\ 1 & \text{else} \end{cases} \tag{13}$$

$$F_5 = \begin{cases} S + \sum_{i=1}^{N} f_{5,i} & \text{if } \sum_{i=1}^{N} f_{5,i} > 0 \\ 0 & \text{if } \sum_{i=1}^{N} f_{5,i} = 0 \end{cases} \tag{14}$$

where $[\beta_{\min}, \beta_{\max}]$ is the range of the slope angle, $\beta_{\max} = \frac{\pi}{4}$, $\beta_{\min} = -\frac{\pi}{4}$ in this article, β_i is the ith slope angle, which is formed by the $(i-1)$th and ith waypoints with:

$$\tan\beta_i = \frac{(z_i - z_{i-1})}{\sqrt{(x_i - x_{i-1})^2 + (y_i - y_{i-1})^2}} \tag{15}$$

To achieve path planning, in the courses of searching for a path by the A* algorithm, adopting the above five objective functions to form the multi-objective function shown in (16), it is constantly considered whether the new adding node satisfies the constraints of the multi-objective function, and uses the above criteria to judge whether a short path does not collide with obstacles and has good smoothness can be obtained.

$$F = F_1 + F_2 + F_3 + F_4 + F_5 \tag{16}$$

2.3 Local Path Planning

2.3.1 Estimated Obstacles Track

In an environment with dynamic obstacles, since the trajectory of the dynamic obstacle is unknown, when the dynamic obstacle is found within the observation radius of the robot, using the autoregressive (AR) prediction method to predict the trajectories of the dynamic obstacle over a period of time, and treating these trajectories as static obstacles in the environment, taking the current position as the origin and the detection range as the radius to search the global path node as the local goal node, then calling the local map and using the improved artificial potential field method to correct the trajectory of the robot to reduce the collision between dynamic obstacles during the movement.

2.3.2 Simulation Comparison of Trajectory Prediction Algorithms

The AR model is chosen as the predict method of the position column of the obstacle since it is simple and fast. For the sake of testing the precision of this method, in a two-dimensional mesh environment with a side length of 1 m and a size of 25 × 25, the Kalman filter method, particle filter method, and AR model are used to estimate the path of the same moving obstacle, that is, the data of the first 16 trajectory points are known, and the data of the last 9 trajectory points are predicted. Actual trajectories of moving obstacles are represented by black solid lines, the predicted tracks are shown by dashed lines, the specific simulation experiments are demonstrated in Fig. 2, and the means square error and calculation time of each predicted path are shown in Table 1 and Fig. 3.

Compared with the other two algorithms, it can be clearly seen that the AR model has the advantages of a simple method, fast algorithm speed, can ensure the accuracy of calculation, and can react and avoid obstacles in a short time when facing dynamic obstacles.

2.3.3 The Improved Artificial Potential Field Algorithm

In most cases, the robot does not have access to all obstacle information under a partially unknown environment, which in turn leads to the global search algorithm cannot complete the path search independently. So, consider local search within a certain range during the robot encounter a partly unknown environment, and decide how to search in virtue of having amended artificial potential field [27] to ensure the route safely.

When dynamic obstacles are observed within the robot's detection range, the artificial potential field method

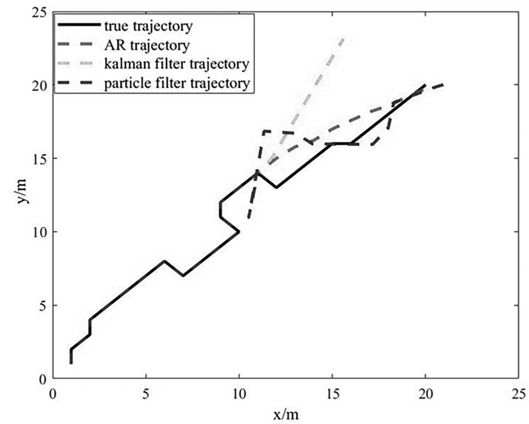

Figure 2. Dynamic obstacle trajectory prediction.

Table 1
Mean Square Error and Calculation Time of Each Predicted Path

	Autoregressive Model	Kalman Filter	Particle Filter
Mean square error	0.1490	0.4455	0.1658
Calculating time	0.2054	0.2150	0.6263

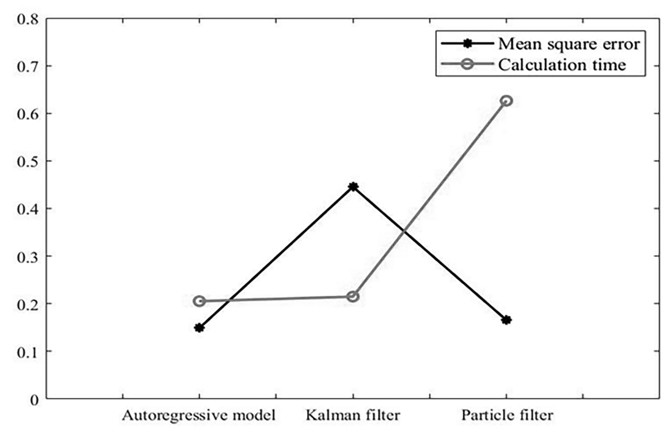

Figure 3. Comparison of relevant data for each prediction path.

is activated to dodge the moving obstacles, and gravity is too large which will lead to a collision with obstacles in the process of barrier avoidance and result in local optimality, so the following improvements are made to gravity in traditional methods:

$$U_{\mathrm{att}} = \begin{cases} \frac{1}{2}\varepsilon\rho^2(P, P_t) & \text{if } \rho(P, P_t) \le l \\ l\varepsilon\rho(P, P_t) - \frac{1}{2}\varepsilon l^2 & \text{otherwise} \end{cases} \tag{17}$$

$$F_{\mathrm{att}} = \begin{cases} \varepsilon(P_t - P) & \text{if } \rho(P, P_t) \le l \\ \frac{l\varepsilon(P_t - P)}{\rho(P, P_t)} & \text{otherwise} \end{cases} \tag{18}$$

where l is a threshold that defines the value of the robot moving away from the obstacle.

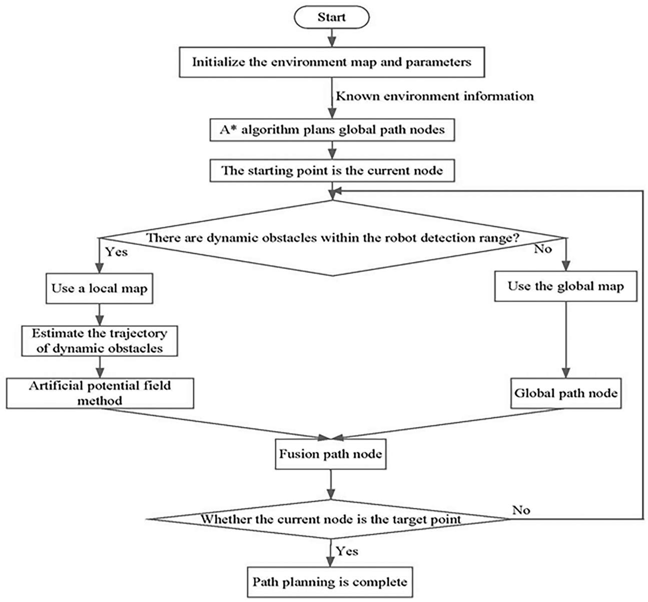

Figure 4. The flowchart of the algorithm.

Similarly, for guarding against the generation of two phenomena: target unreachable and local optimum, gravitational guidance factors are added to the repulsive potential field to generate a force from the robot pointing to the destination at the same time as the repulsive force, which in turn can properly drag the robot away from the obstacle, in addition, gravitational force and repulsive force can simultaneously become zero when the robot reaches the goal node, avoiding the problem of the target being unreachable, repulsion and repulsive potential field are improved as follows:

$$U_{rep} = \begin{cases} \frac{1}{2}\eta\left(\frac{1}{D_{\min}(P_i)} - \frac{1}{r}\right)^2 \rho_t^2 & \text{if } D_{\min}(P_i) \le r \\ 0 & \text{otherwise} \end{cases} \tag{19}$$

$$F_{rep} = \begin{cases} \eta\left(\frac{1}{D_{\min}(P_i)} - \frac{1}{r}\right) \frac{\rho_t^2 \nabla D_{\min}(P_i)}{D_{\min}^2(P_i)} + \eta\left(\frac{1}{D_{\min}(P_i)} - \frac{1}{r}\right)^2 \rho_t & \text{if } D_{\min}(P_i) \le r \\ 0 & \text{otherwise} \end{cases} \tag{20}$$

2.3.4 Local Map Segmentation

When the robot's radar detects a dynamic obstacle, it regards its current location as the origin point and uses the radar detection radius as the basis for finding the local target point, that is, looking for the local path point in the set of global route point from where the robot is currently located. The predicted dynamic obstacle trajectory position is used as a static obstacle, and the original static obstacle in the current local map is considered, after completing the local pathfinding with the modified artificial potential field method, go back to the global roadway point and repeat the above operations until a holonomic path is found.

2.4 The Fusion of Algorithms

The integration of global and local route search is realised by utilising the modified A* algorithm and artificial potential field method, namely, MAAPF, to avoid that the global path planning has poor dynamic barrier avoidance ability and local path planning easily falls into local optimal. In the beginning, the improved A* algorithm is implemented to search the route node to be added. Assuming that the mobile obstacle is found within the observation radius of the mobile robot at the nth point, the artificial potential field method is used to calculate the route in the local map. In fact, use a local map and only consider static obstacles within this range in the path planning of dynamic obstacle avoidance, rather than use the global map, which is more conducive to saving calculation time and improving the efficiency of finding paths by reducing the number of times the global map was called. The flowchart for the fusion algorithm is displayed in Fig. 4.

3. The Simulation in the Dynamic and Static Environments

The simulation of the robot path planning is conducted through MATLAB on a Windows10 operating system. Before the experiment starts, the robot is regarded as a point with the preestablished initial movement direction in a 3D environment map with 92 obstacles distributed as shown in Fig. 5, the start position and endpoint are also predefined and marked in the environment with red and blue circles, respectively. The simulation of the improved A* algorithm with other algorithms is shown in Fig. 5(a) and (b), at the same time, as exhibited in Fig. 5(c), the availability of the improved algorithm is also confirmed by gradually increasing the constraint function.

In a 21 × 21 map, selects initial point is (1, 1) and the goal location is (20, 20), through multiple iteration calculations, the comparison of path length, convergence time, and other data are revealed in Table 2, a line chart of Fig. 6 is also plotted using the data in Table 2. After contrast, it is found that the overall performance of improving A* algorithm outperforms other algorithms. In the actual robot operation process, fewer path points and path steering points can reduce the excessive energy consumption caused by robot steering, and have high use value, which indicates that the improved A* algorithm has strong practicality.

To further validate the feasibility of the improved artificial potential field method, in the 21 × 21 map with (0, 0) as the starting point and (20, 20) as the endpoint marked by a red triangle, selecting the four dynamic obstacles with different directions and velocities and a radius of 0.4, at the same time regards robot as a particle during the movement process, comparing the dynamic obstacle avoidance effect of the conventional, the improved artificial potential field method and the artificial potential filed with escape force, and the overall path diagram of the specific policy is shown in Fig. 7,

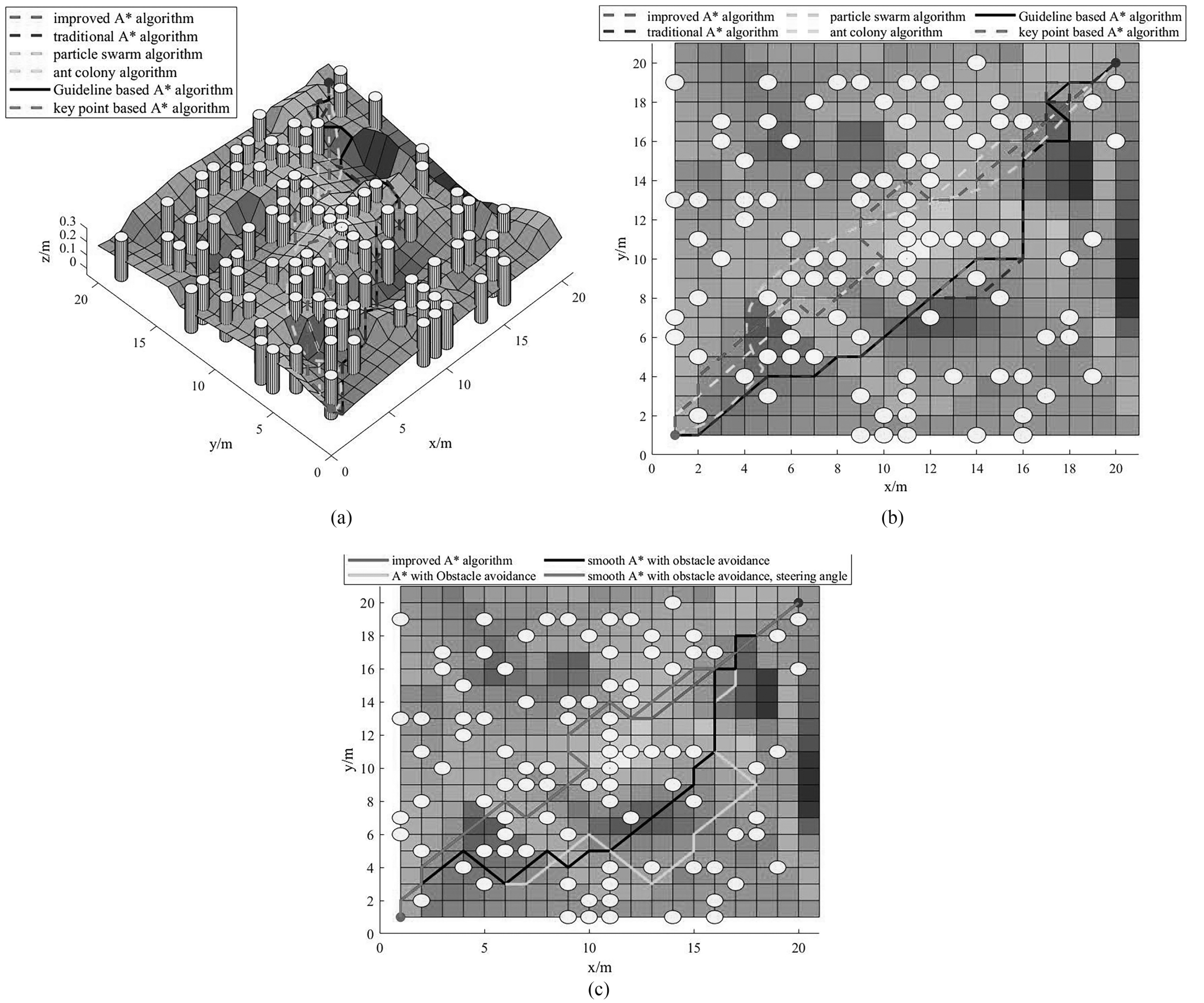

Figure 5. The path comparative simulation: (a) the 3D path comparative simulation; (b) the comparison of the 2D projective path; and (c) the comparison of variants of other A* algorithms.

Table 2
Relevant Data for Algorithm Comparison in Fig. 5

	Path Length	Convergence Time	Turning Points of the Path	Number of Route Points
Traditional A* algorithm	31.5916	32.5880	14	25
Improved A* algorithm	32.3184	31.8315	11	25
Particle swarm algorithm	31.2189	120.5407	3	28
Ant colony algorithm	30.6274	103.5875	11	25
Guideline based A* algorithm	32.4163	37.4007	14	28
Key point based A* algorithm	31.5921	37.1364	11	28
A* with obstacle avoidance	39.1461	36.7962	13	31
Smooth A* with obstacle avoidance	34.6594	37.1484	14	29
Smooth A* with obstacle avoidance, steering angle	32.3186	36.2608	12	25

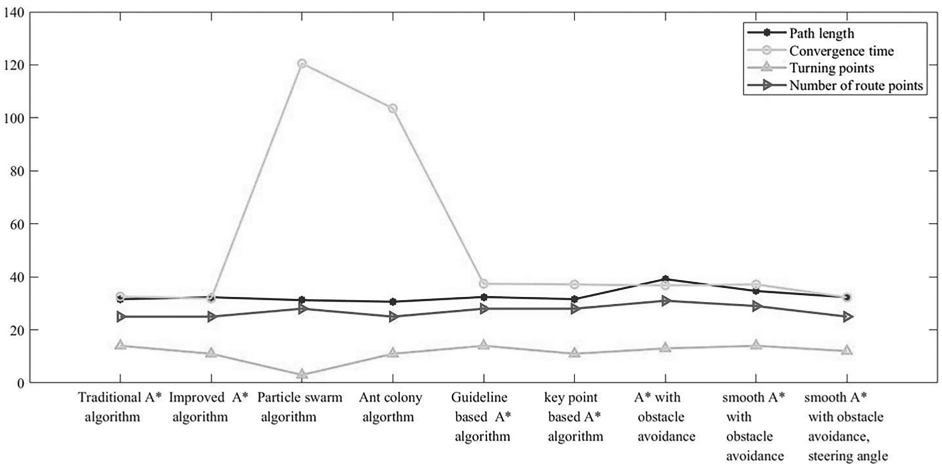

Figure 6. Comparison chart of related data for the algorithm.

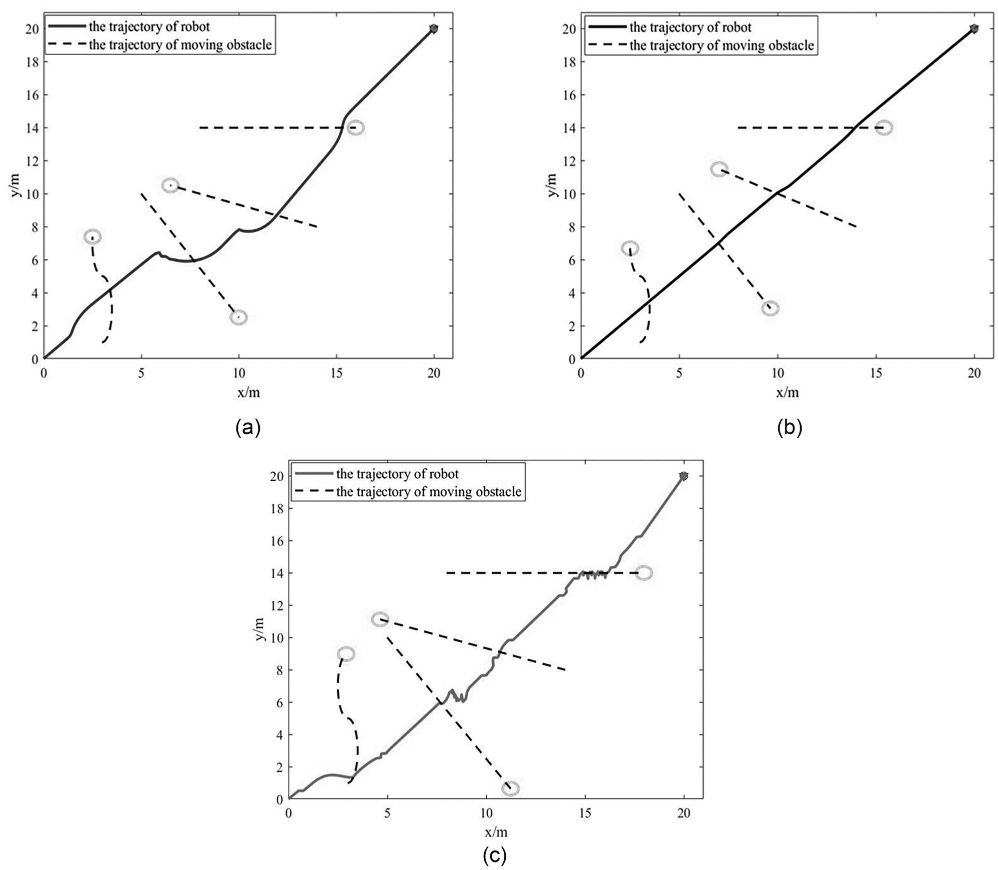

Figure 7. The simulation of avoiding the moving obstacles: (a) the improved artificial potential field; (b) the conventional artificial potential field; and (c) the artificial potential field with escape force.

the initial speed and position of the obstacles are in Table 3.

In the simulation of dynamic obstacle avoidance, the dotted line represents the track of the green moving obstacle, and the solid blue, black, and purple lines, respectively, represent the trajectory of the robot by applying the modified, conventional artificial potential field, and artificial potential field method with escape force.

Figure 8 further illustrates the effect of the improved artificial potential field to elude the moving obstacle, which can be clearly observed that the modified artificial potential field can better keep away from each moving obstacle, while the conventional artificial potential field is able to avoid the first dynamic obstacle, but collides with the subsequent moving obstacles. Although the method in Fig. 8(c) can avoid the second and third dynamic obstacles, it will also collide with the first and last obstacles. From the above simulation diagrams, it can be clearly seen that the improved artificial potential field method has good obstacle avoidance ability.

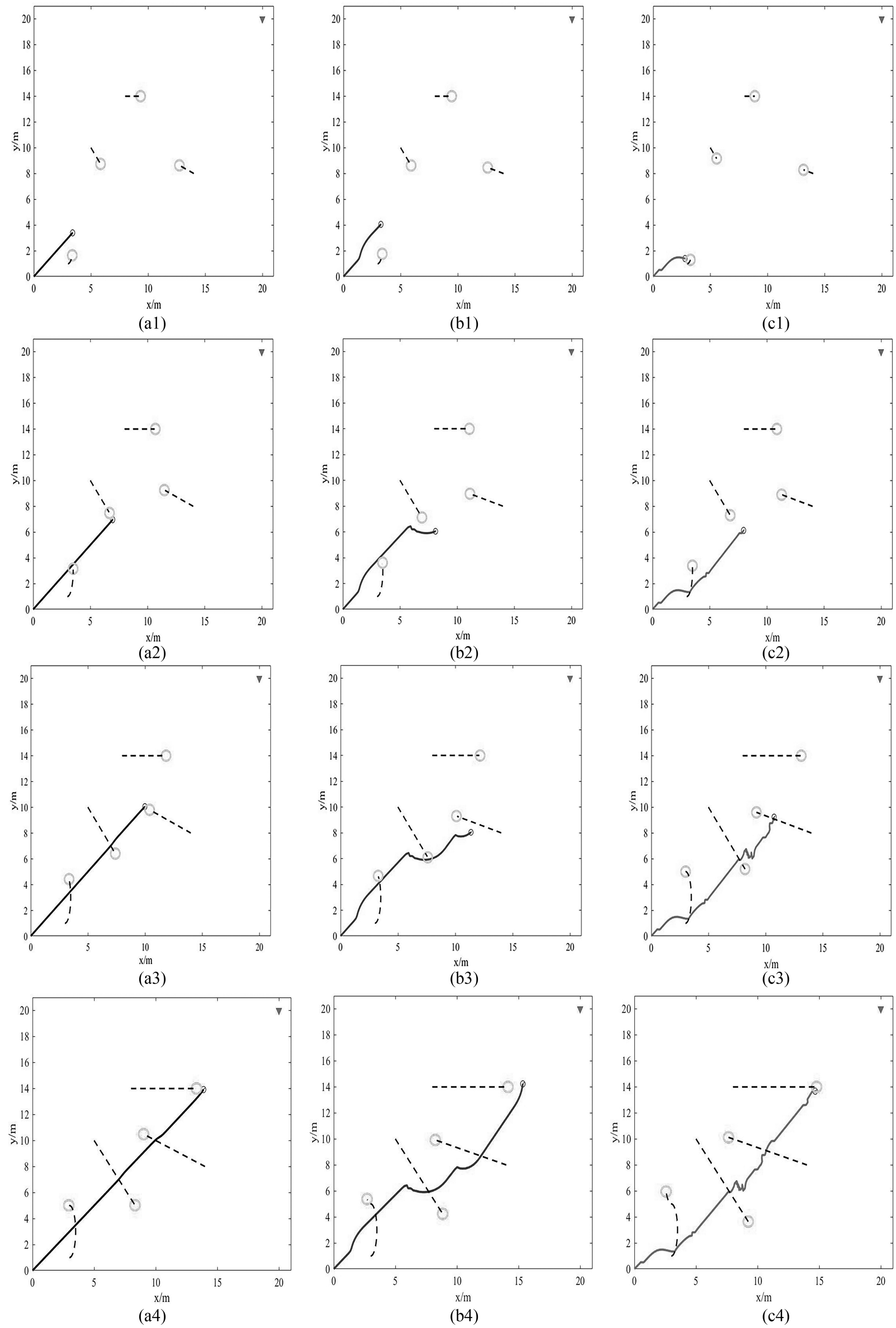

Figure 8. Obstacle avoidance comparing of different dynamic obstacles: (a) the conventional artificial potential field method; (b) the improved artificial potential field method; and (c) the artificial potential field method with escape force.

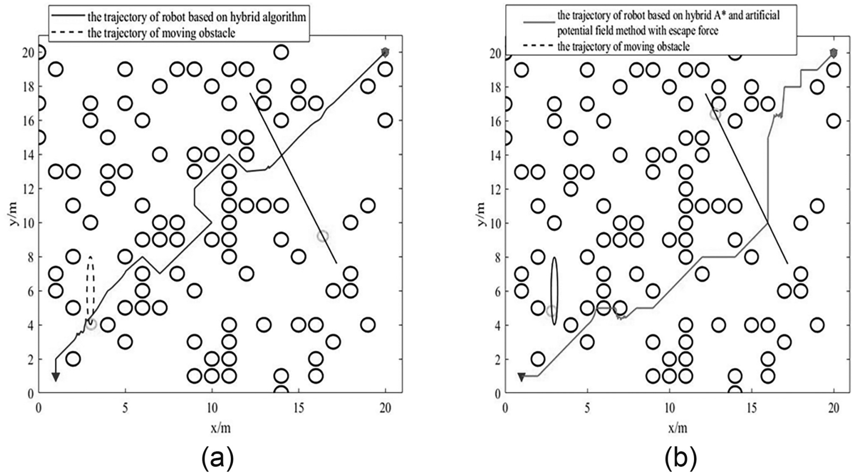

Figure 9. Dynamic obstacle avoidance simulation.

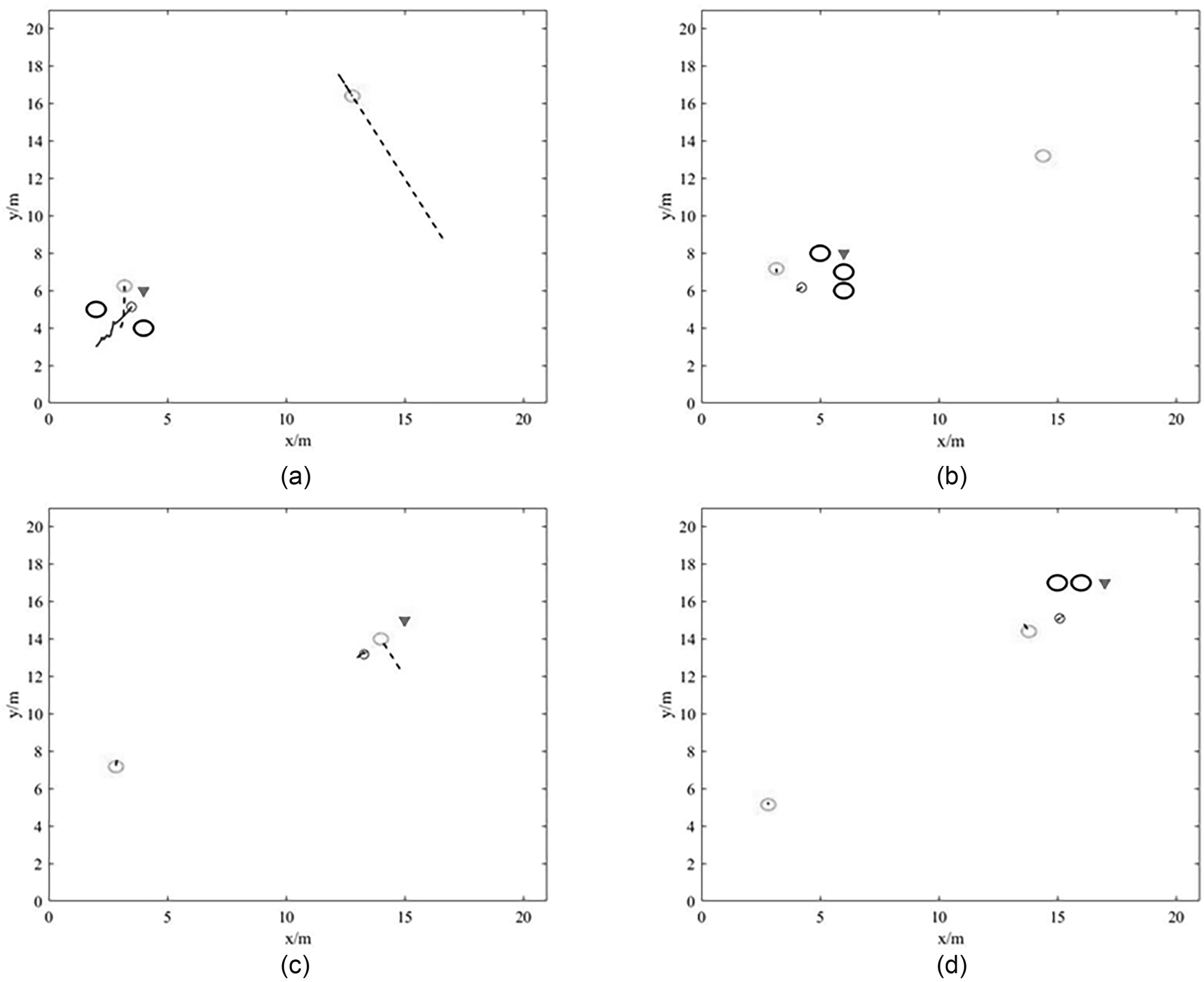

Figure 10. Local pathfinding simulation of moving obstacles based on the hybrid algorithm in this paper. (a)–(d) local map when encountering dynamic obstacles.

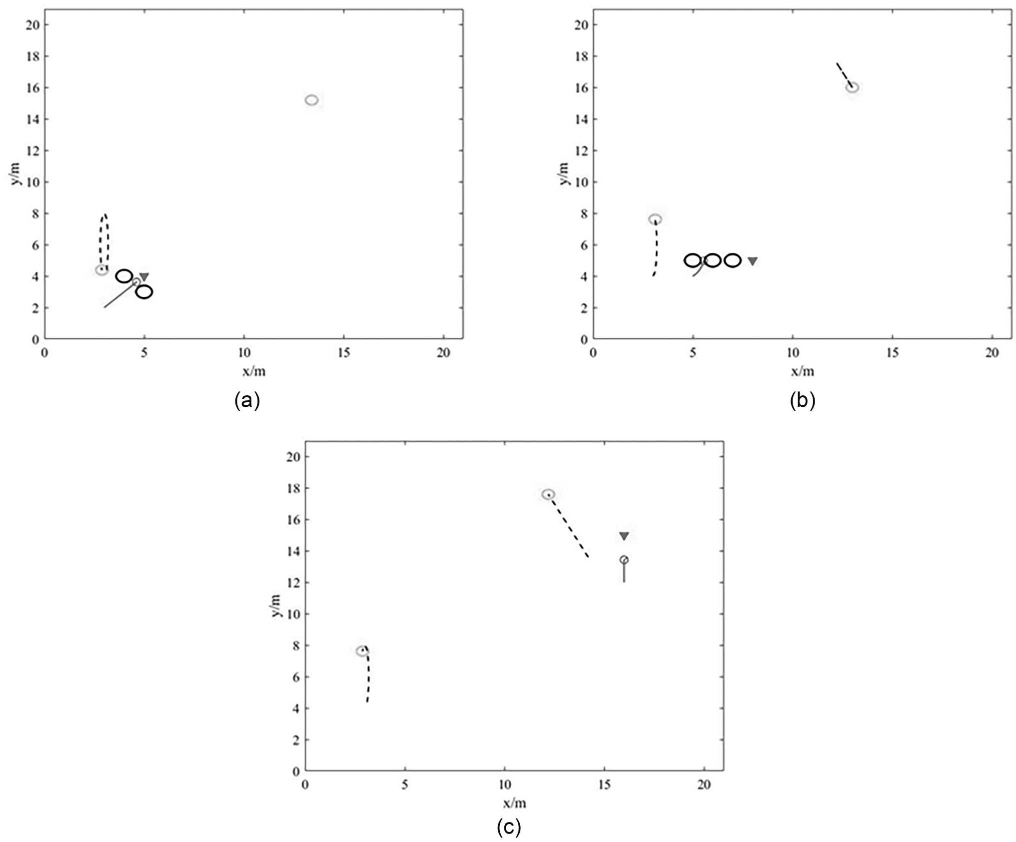

Figure 11. Local pathfinding simulation of moving obstacles based on the hybrid A* and artificial potential field method with escape force: (a)–(c) local map when encountering dynamic obstacles.

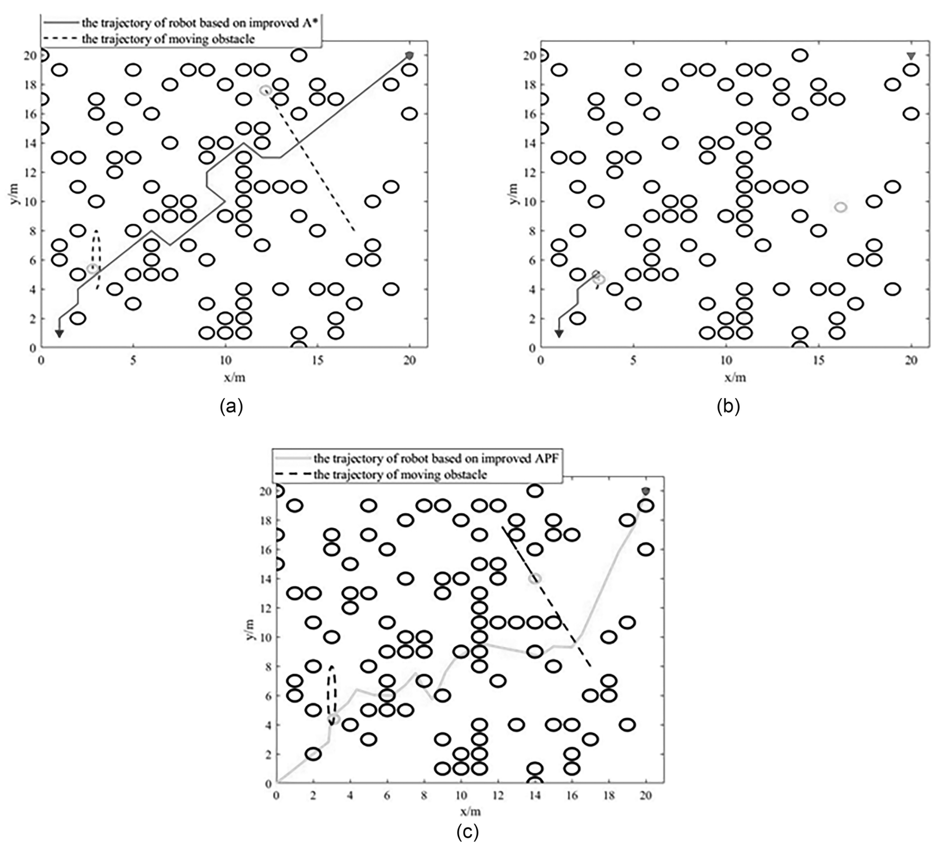

Figure 12. Simulation of a single algorithm in a complex environment: (a) and (b) the improved A* algorithm; and (c) the improved artificial potential field method.

Table 3
Initial Position and Speed of Dynamic Obstacles in Figs. 7 and 8

Initial Position	Speed Direction	Speed (m/s)
(8,14)	$\overrightarrow{(20.8, 14)}$	(0.064, 0)
(3,1)	$\overrightarrow{(14, 15)}$	(0.4990, 0.1255)
(5,10)	$\overrightarrow{(13, -2)}$	(0.04, −0.06)
(14,8)	$\overrightarrow{(2, 14)}$	(−0.06, 0.03)

Table 4
Initial Position and Speed of Dynamic Obstacles in Figs. 9–12

Initial Position	Speed Direction	Speed (m/s)
(3,4)	$\overrightarrow{(3,\ 8)}$	(0.0284, 0.2558)
(17,8)	$\overrightarrow{(12.2,\ 17.6)}$	(−0.2, 0.4)

To confirm the availability of the fusion algorithm in the circumstance with dynamic obstacles, also with (1, 1) as the starting point and (20, 20) as the endpoint for simulation experiments in the 21×21 map, on the basis of the original 97 static obstacles, the static obstacles located at (15, 11) are set as dynamic obstacles with (17, 8) as the starting point for round-trip movement, and another dynamic makes a curved movement, the corresponding position and speed are exhibited in Table 4, at the same time, the hybrid algorithm based on A* and artificial potential field with escape force is applied to this scenario and compared with the hybrid algorithm in this paper, the effects of global and local path planning are revealed in Figs. 9 and 10.

In Fig. 9, the smaller green circle is a dynamic obstacle, the opposite static obstacle is black circle and the black dotted line is its trajectory because the two dynamic obstacles move back and forth, so the trajectory of the second dynamic obstacle is finally presented as a solid black line. Figs. 10 and 11 are the simulation results of local path planning when the robot comes across three dynamic obstacles, the red triangle represents the local target point, and it can be noticed from the above figures that the hybrid algorithm can effectively avoid obstacles in circumstances with dynamic obstacles and find the global path, and another path planned by the hybrid A* algorithm and the artificial potential field method with escape force is not feasible.

In Fig. 12, the simulation figures with label (a) and label (b) are the path planning results of the improved A* algorithm in a complex environment, and the solid red line is the final planned path, but in the process of planning, its path collides with the first moving obstacle. The simulation figure with label (c) is the simulation result of the improved artificial potential field method in a complex environment, through the solid blue line of the lake is the final path, and the planned path is not feasible. Compared to Fig. 9(a), it can be clearly seen that the complete path can be planned in the case of mixing the two algorithms and avoiding the obstacle successfully.

4. Conclusions

For purpose of further realizing the pathfinding in the circumstance with dynamic obstacles, improve the poor obstacle avoidance ability of global route search and the characteristics of local route search that is easy to fall into local optimisation, the MAAPF which is a fusion scheme of A* algorithm and artificial potential field method is provided. The trajectory planning of a single robot in circumstances with dynamic obstacles can obtain the optimal smooth path from a predetermined starting point to an ending point and effectively avoid dynamic obstacles in the environment. Introducing the multi-objective function in the A* algorithm to avoid producing too many redundant points, meanwhile, for averting the matter of local optimality and unattainable target in the local map, ameliorating the artificial potential field method by setting the gravitational threshold and gravitational guidance factor. Through simulation, the improved A* technology can find the path faster than other algorithms (such as PSO, ant colony algorithm, and other variants of A* algorithm), there are fewer turning points than the traditional A* algorithm, and the improved artificial potential field method has better ability to avoid obstacles in the area where there are dynamic obstacles.

Acknowledgement

This research was funded by the National Science Foundation for Young Scientists of China (51909049), Start-up funds for doctoral and master's research (217045338).

References

[1] L. Liu, J. Yao, D. He, J. Chen, J. Huang, H. Xu, B. Wang, and J. Guo, Global dynamic path planning fusion algorithm combining jump-A* algorithm and dynamic window approach, *IEEE Access*, *9*, 2021, 19632–19638.

[2] D. Zhu, C. Tian, B. Sun, and C. Luo, Complete coverage path planning of autonomous underwater vehicle based on GBNN algorithm, *Journal of Intelligent and Robotic Systems*, *94*(1), 2019, 237–249.

[3] L. Zhang, Y. Zhang, and Y. Li, Mobile robot path planning based on improved localized particle swarm optimization, *IEEE Sensors Journal*, *21*(5), 2021, 6962–6972.

[4] Y. Zhang and S. Wang, LSPP: A novel path planning algorithm based on perceiving line segment feature, *IEEE Sensors Journal*, *22*(1), 2022, 720–731.

[5] L. Lacasa, B. Luque, F. Ballesteros, J. Luque, and J.C. Nuo, From time series to complex networks: The visibility graph, *Proceedings of the National Academy of Sciences*, *105*(13), 2008, 4972–4975.

[6] D. Wang, Indoor mobile robot path planning based on improved A* algorithm, *Journal of Tsinghua University (Science and Technology)*, *52*, 2012, 1085–1089.

[7] Q. Jin, C. Tang, and W. Cai, Research on dynamic path planning based on the fusion algorithm of improved ant colony optimization and rolling window method, *IEEE Access*, *10*, 2021, 28322–28332.

[8] Z. Wang, G. Li, and J. Ren, Dynamic path planning for unmanned surface vehicle in complex offshore areas based

on hybrid algorithm, *Computer Communications*, *166*, 2021, 49–56.
[9] W. Shan and Z. Meng, Design of smooth path based on improved A* algorithm, *Journal of Southeast University (Natural Science Edition)*, *40*(S1), 2010, 155–161.
[10] Z. Qin, X. Chen, M. Hu, L. Chen, and J. Fan, A novel path planning methodology for automated valet parking based on directional graph search and geometry curve, *Robotics and Autonomous Systems*, *132*, 2020, 103606.
[11] C. Lin, H. Wang, J. Yuan, and M. Fu, An online path planning method based on hybrid quantum ant colony optimization for AUV, *International Journal of Robotics and Automation, 33*(4), 2018, 435–444.
[12] B. Fu, L. Chen, Y. Zhou, D. Zheng, Z. Wei, J. Dai, and H. Pan, "An improved A* algorithm for the industrial robot path planning with high success rate and short length," *Robotics and Autonomous Systems*, *106*, 2018, 26–37.
[13] X. Zhong, J. Tian, H. Hu, and X. Peng, Hybrid path planning based on safe A* algorithm and adaptive window approach for mobile robot in large-scale dynamic environment, *Journal of Intelligent and Robotic Systems*, *99*(1), 2020, 65–77.
[14] H. Wang, S. Lou, J. Jing, Y. Wang, W. Liu, and T. Liu, The EBS-A* algorithm: An improved A* algorithm for path planning, *PLoS One*, *17*(2), 2022, e0263841.
[15] Z. Chen, Y. Zhang, Y. Zhang, Y. Nie, J. Tang, and S. Zhu, A hybrid path planning algorithm for unmanned surface vehicles in complex environment with dynamic obstacles, *IEEE Access*, *7*, 2019, 126439–126449.
[16] H. Wang, C. Hao, P. Zhang, M. Zhang, P. Yin, and Y. Zhang, Path planning of mobile robots based on A* algorithm and artificial potential field method, *China Mechanical Engineering*, *30*(20), 2019, 2489–2496.
[17] F. Duchoň, A. Babinec, M. Kajan, P. Beňo, M. Florek, T. Fico, and L. Jurišica, Path planning with modified a star algorithm for a mobile robot, *Procedia Engineering*, *96*, 2014, 59–69.
[18] X. Ji, S. Feng, Q. Han, H. Yin, and S. Yu, Improvement and fusion of A* algorithm and dynamic window approach considering complex environmental information, *Arabian Journal for Science and Engineering*, *46*(8), 2021, 7445–7459.
[19] Z. Liu, H. Liu, Z. Lu, and Q. Zeng, A dynamic fusion pathfinding algorithm using delaunay triangulation and improved a-star for mobile robots, *IEEE Access*, *9*, 2021, 20602–20621.
[20] Y. Guo, Q. Liu, J. Bao, F. Xu, and W. Lv, Review of research on AUV obstacle avoidance algorithms based on artificial potential field method, *Computer Engineering and Applications*, *56*(4), 2020, 8.
[21] J. Yu, W. Deng. Z. Zhao, X. Wang, J. Xu, L. Wang, Q. Sun, and Z. Shen, A hybrid path planning method for an unmanned cruise ship in water quality sampling, *IEEE Access, 7*, 2019, 87127–87140.
[22] X. Wang, L. Yang, Y. Zhang, and S. Meng, Robot path planning based on improved ant colony algorithm with potential field heuristic, *Control and Decision*, *33*(10), 2018, 7.
[23] S. Zhu, W. Zhu, X. Zhang, and T. Cao, Path planning of lunar robot based on dynamic adaptive ant colony algorithm and obstacle avoidance, *International Journal of Advanced Robotic Systems, 17*(3), 2020, 4149–4171.
[24] J. Li, B. Xu, Y. Yang, and H. Wu, Three-phase qubits-based quantum ant colony optimization algorithm for path planning of automated guided vehicles, *International Journal of Robotics and Automation, 34*(2), 2019, 156–163.
[25] D. Zhu, C. Cheng, and B. Sun, An integrated AUV path planning algorithm with ocean current and dynamic obstacles, *International Journal of Robotics and Automation, 31*(5), 2016, 382–389.
[26] P. Das, H. Behera, S. Das, H. Tripathy, B. Panigrahi, and S. Pradhan, A hybrid improved PSO-DV algorithm for multi-robot path planning in a clutter environment, *Neurocomputing*, *207*, 2016, 735–753.
[27] B. Kovács, G. Szayer, F. Tajti, M. Burdelis, and P. Korondi, A novel potential field method for path planning of mobile robots by adapting animal motion attributes, *Robotics and Autonomous Systems*, *82*, 2016, 24–34.

Biographies

Chongyang Lv received his B.S. degree in mathematics from Northeast Forestry University in 2010, his M.Sc. degree and Ph.D. degree from Harbin Engineering University in 2013 and 2018. At present, he is a lecturer at the School of Science, Harbin University of Science and Technology. His research interest includes multi-agent path planning, collaborative control and navigation of multiagent (robot), and artificial intelligence algorithms.

Xuejie Fan received her B.S. degree in Mathematics and Applied Mathematics from Binzhou University. She is currently pursuing an M.Sc. degree in Mathematics at Harbin University of Science and Technology. Her research interest includes robot path planning and artificial intelligence calculation method.

Mingxiao Sun received his B.E. and Ph.D. degrees from the College of Automation, Harbin Engineering University respectively in 2010 and 2018. He is currently an Associate Professor in School of Automation, Harbin University of Science and Technology. His research interest includes group system path planning and ship motion control.